



HAL
open science

THE EFFECTS OF IMAGE GAS ON ATOM PROBE ANALYSIS

M. Miller, K. Russell

► **To cite this version:**

M. Miller, K. Russell. THE EFFECTS OF IMAGE GAS ON ATOM PROBE ANALYSIS. Journal de Physique Colloques, 1988, 49 (C6), pp.C6-81-C6-86. 10.1051/jphyscol:1988614 . jpa-00228111

HAL Id: jpa-00228111

<https://hal.science/jpa-00228111>

Submitted on 4 Feb 2008

HAL is a multi-disciplinary open access archive for the deposit and dissemination of scientific research documents, whether they are published or not. The documents may come from teaching and research institutions in France or abroad, or from public or private research centers.

L'archive ouverte pluridisciplinaire **HAL**, est destinée au dépôt et à la diffusion de documents scientifiques de niveau recherche, publiés ou non, émanant des établissements d'enseignement et de recherche français ou étrangers, des laboratoires publics ou privés.

THE EFFECTS OF IMAGE GAS ON ATOM PROBE ANALYSIS

M.K. MILLER and K.F. RUSSELL

*Metals and Ceramics Division, Oak Ridge National Laboratory,
Oak Ridge, TN 37831-6376, U.S.A.*

Abstract - The effects of image gas pressure on the performance of an energy-compensated atom probe have been investigated. The results indicate that the quantitative accuracy of the composition determinations is seriously degraded at gas pressures typically used during field-ion imaging. The mass resolution is degraded both in terms of the increase in the width of the peaks in the spectra and also in the number of ions in the tails of the peaks. The number of afterpulses is also increased.

1. INTRODUCTION

In addition to improving the mass resolution of an atom probe, the incorporation of an energy-compensating lens makes it possible in principle to perform elemental analysis while viewing the field-ion image without significantly increasing the low background noise level. In an energy-compensated atom probe, the lens is set to transmit only ions with the energy of the standing plus pulse voltages. The random noise from the image gas forming the field-ion image and projected from the specimen is filtered out because these gas ions have only the standing component of the voltage. Therefore, these ions are not transmitted through the energy-compensating lens to the detector. Field adsorbed image gas atoms on the surface of the specimen can be desorbed with the energy of the standing plus pulse voltages and will produce an additional set of peaks in the spectrum at the mass-to-charge ratios characteristic of the image gas rather than as random background noise. These additional peaks are ignored in the compositional determinations. The background neutral image gas atoms in the vacuum system do not have sufficient energy to produce a signal at the detector. However, the presence of these gas atoms will affect the performance of the instrument through several other processes. The effects of the image gas may be separated into 3 main categories: 1) those affecting the field ionization and evaporation processes at the specimen, 2) those affecting the probability of a genuine ion from the specimen colliding with or being deflected by a gas atom during its flight through the drift tubes and the energy-compensating lens, and 3) those affecting the performance of the single atom detector.

In this paper, the results of a systematic study of the performance of an energy-compensated atom probe as a function of image gas pressure are reported. The scope of the discussion will focus on the results of image gas pressure on atom probe performance and the definition of the experimental constraints for quantitative compositional analysis. The physical processes responsible for the changes in performance will be discussed in more detail in a subsequent paper.

2. EXPERIMENTAL

The three inert image gases investigated in this study were helium, neon, and argon. The image gas pressure was varied between the background base pressure and 1×10^{-3} mBar. The highest pressure used was the maximum possible experimentally because of potential electrical breakdown in the single atom detector. All pressures quoted in this paper have been corrected with the appropriate ion gauge factors. The background base pressure for all analyses was between 2 and 8×10^{-11} mBar. Although a static vacuum was maintained during analysis, the reactive gases were controlled with a titanium sublimation pump. In addition to the type and pressure of image gas present during analysis, the following experimental conditions were also varied: specimen temperature, pulse fraction, voltage settings of the energy-compensating lens, beam divergence, and specimen position. It should be noted that the specimen temperature range for argon was limited to greater than -80 K due to condensation of the image gas on the cryostat. Therefore, in order to compare image gases directly under constant conditions, temperatures higher than 80 K were used.

The material used for this series of experiments was a homogeneous Ni₃Al-based alloy containing 23.5 at. % Al, 0.5 at. % Hf, and 0.24 at. % B. This alloy was selected because of the relatively wide mass range that these elements span [mass-to-charge ratios between 5 and 64 atomic mass units (amu)], the wide separation of the mass peaks, the absence of any isobar and charge state overlaps, and the stability of this material to field evaporation. All compositions are quoted in atomic percent.

All atom probe analyses were performed in the ORNL energy-compensated instrument.^[1] This atom probe features a double channel plate detector and a flight path from specimen to detector of 2.26 m. Two high voltage mercury-wetted pulsers were used with pulse widths of either 7 or 17 ns. The high voltage pulse repetition rate

was 50 Hz. The ORNL-designed high speed digital timing system features a Phillips Scientific 6854 preamplifier with a 1 GHz bandwidth and a LeCroy 4208 multihit time-to-digital converter with 1 ns resolution. The double pulse pair resolution of this system is 2 ns. The full width at half maximum (FWHM) parameters were determined from the major Al^{++} and $^{58}Ni^{++}$ peaks in the time spectra at mass-to-charge ratios of 13.5 and 29 amu, respectively. Compositions were generally determined from data blocks containing a minimum of 10,000 ions that were taken under constant experimental conditions. However, in some adverse conditions, particularly at high gas pressures, collecting this number of atoms was not practical.

3. RESULTS AND DISCUSSION

3.1 Composition Determinations

The apparent measured composition was found to depend on the image gas pressure and the type of image gas. The apparent levels of aluminum, hafnium and boron are plotted in Fig. 1 as a function of helium, neon and argon image gas pressures. A 20% pulse ratio was used for this set of analyses. It should be noted that these data sets were taken with a specimen temperature of 100 K and therefore some preferential evaporation and retention was likely to occur. The apparent aluminum level increased slightly with increasing helium pressure. A similar slight increase in apparent aluminum level was observed with neon up to 10^{-4} mBar, but above this pressure a dramatic increase in the apparent aluminum level occurred. In the case of argon, a slight increase was observed up to 10^{-6} mBar at which point a marked decrease in the apparent aluminum level occurred. Pressures higher than 10^{-4} mBar were not experimentally practical with argon due to the significant increase in background noise and poor transmission of genuine specimen ions to the detector. The trends were more difficult to distinguish in the case of hafnium and boron because of the relatively larger error of the readings due to the smaller number of ions detected. No systematic change was observed for the highest mass element hafnium. In the case of boron, a small decrease in the apparent level was observed with helium whereas no clear trend was evident with either neon or argon.

3.2 Pulse Fraction Effects

The image gas pressure was found to have a relatively small influence on the preferential evaporation and retention of the elements as shown in Fig. 2. These data indicated that preferential evaporation of the nickel was occurring since the measured aluminum content increased with smaller pulse fractions. The effect was slightly more severe at higher image gas pressures. It should also be emphasized that reducing the pressure from 10^{-9} to 10^{-11} mBar made it necessary to increase the potential on the specimen by almost 20% to maintain the same ion collection rate at the single atom detector. At higher gas pressures no such increase was required thus indicating, as expected, that the presence of image gas is influencing the field evaporation process at the specimen.

3.3 Time Resolution and Afterpulsing

The performance of the ORNL-designed digital timing system was evaluated to ensure that it was not the limiting factor for the subsequent analyses. It has been shown previously in a similar instrument that the FWHM of the time spectra peaks is improved at small beam divergences.^[2] Therefore, the performance of the system was determined with the minimum beam divergence of 13 mrad. The normalized Al^{++} and Ni^{++} peaks taken with this small beam divergence and in the presence of neon at 10^{-7} mBar with a 20% pulse ratio and a specimen temperature of 50 K are shown in Fig. 3.¹ Under these experimental conditions, the FWHM was measured as <2 ns and the full width at the base of the peak was 5 ns. These results indicated that the time resolution of the instrument was sufficient to observe the influences of image gas on the spectra. It should be noted that the VG-designed 163° sector energy-compensating lens is not a true Poschenreider configuration since the electrodes feature only a single radius of curvature. However, two sets of five fringe field electrodes are used to compensate for the single radius of curvature by modifying the field gradients in the energy-compensating lens. No significant difference in performance was observed by altering the position of the specimen by ± 1 cm from the normal position along the ion-optical axis.

Three sets of data taken with the maximum beam divergence of 36 mrad, a specimen temperature of 100 K, a pulse ratio of 20%, and in the presence of 10^{-8} , 2×10^{-4} , and 6×10^{-8} mBar of neon are shown in Fig. 4. Similar data sets for helium at 2×10^{-4} and 8×10^{-8} mBar and argon at 10^{-8} and 10^{-4} mBar are shown in Figs. 5 and 6, respectively. The peak shapes were found to be symmetrical about the midpoint with approximately equal number of ions found in the high-time and low-time tails. For all image gases, the number of ions in both the high-time and low-time tails of the peaks increased with higher image gas pressures. Relatively little difference in the FWHM of the peaks was observed at pressures below 10^{-6} mBar. The peaks recorded with pressures in the 10^{-8} mBar range are representative examples of the form of these lower pressure results. At higher pressures, the width of the peaks expanded rapidly with increasing pressure.

The number of afterpulses produced in the single atom detector was also found to increase at the higher pressures. It is often suggested that to minimize ion pile-up effects at the detector the energy-compensating lens should be slightly defocused to deliberately detune the mass spectrometer. A consequence of this method at gas

¹In Figs. 3 to 6, the abscissa is the difference in time from the flight time of the central peak.

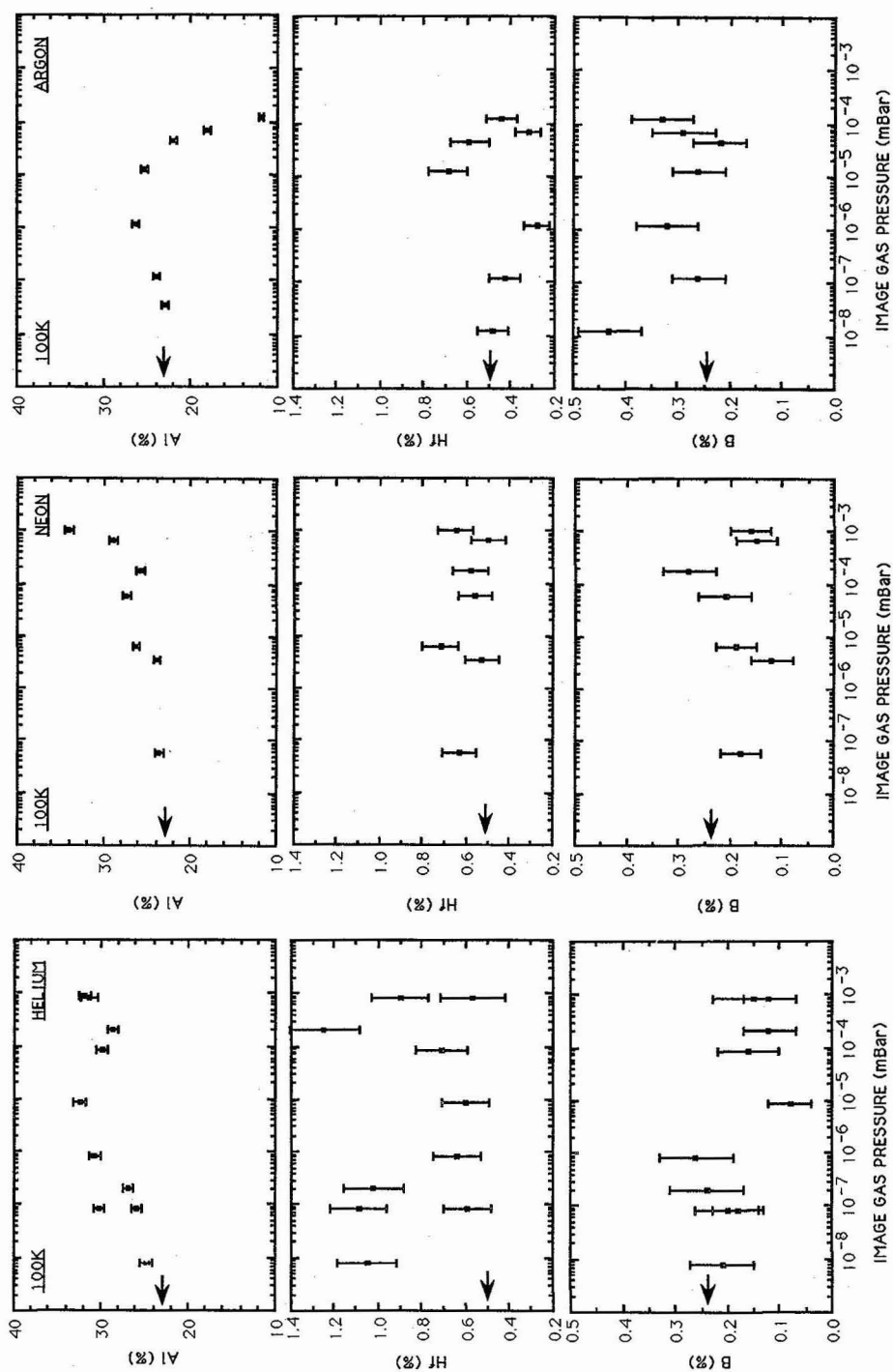


Fig. 1. Variations in apparent aluminum, hafnium, and boron levels with helium, neon, and argon gas pressures.

pressures greater than 10^{-6} mBar, particularly in the case of argon, is to increase the number of afterpulses produced. Since these afterpulses are generated primarily as a result of ionizing adsorbed atoms on the surface of the channels in the detector, increasing the image gas pressure or allowing the image gas to reestablish the adsorbed layer on the channels will increase the quantity of afterpulses. When the ion beam is focused to a small spot on the detector the same channels are used repeatedly and the secondary electrons produced flush the channels of gas atoms and prevent the establishment of an adsorbed gas layer in these channels. If the beam covers a larger number of channels this flushing process will not prevail and the number of adsorbed gas atoms in the channels will increase and therefore produce a larger number of afterpulses.

3.4 Recommended Operating Conditions

These experiments have indicated that the optimum performance of an energy-compensated atom probe is achieved with the minimum of image gas present. Therefore, distance-monitored analyses should be performed with the lowest gas pressure which allows the collapse of planes to be observed. A slight degradation in performance is observed up to approximately 10^{-6} mBar. The presence of a limited pressure of image gas may be beneficial in some situations since the field that has to be applied to field evaporate atoms from the specimen surface is reduced. Pressures above 10^{-6} mBar should be avoided.

4. CONCLUSIONS

These results have indicated that, at the typical image gas pressures where field-ion images are normally obtained, the mass resolution of the atom probe is seriously degraded both in terms of the FWHM of the mass spectra and the increased number of ions in the tails of the mass spectra, the number of afterpulses produced in the single atom detector is increased, and the accuracy of the compositional determination is affected. It is therefore recommended that atom probe analyses be performed with the minimum of image gas present.

5. Acknowledgment

The authors would like to thank Dr. G. D. W. Smith of Oxford University and Dr. M. G. Hetherington of M. I. T. for helpful discussions. This research was sponsored by the Division of Materials Sciences, U.S. Department of Energy, under contract DE-AC05-84OR21400 with Martin Marietta Energy Systems, Inc.

6. REFERENCES

1. M.K. Miller, *J. de Physique*, **47-C2**, (1986) 493
2. A. Cerezo, G.D.W. Smith and A.R. Waugh, *J. de Physique*, **45-C9**, (1984) 329

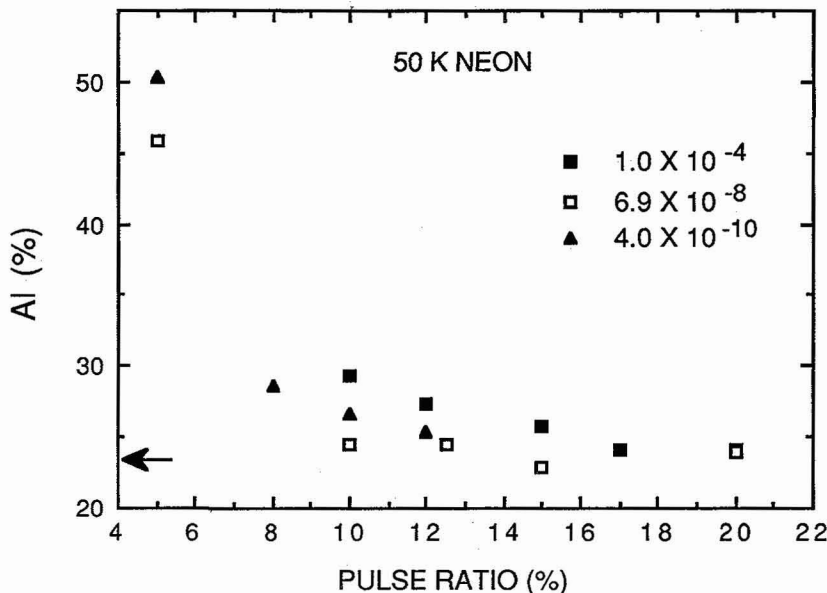


Fig. 2. Effect of pulse ratio and image gas pressure on apparent aluminum composition.

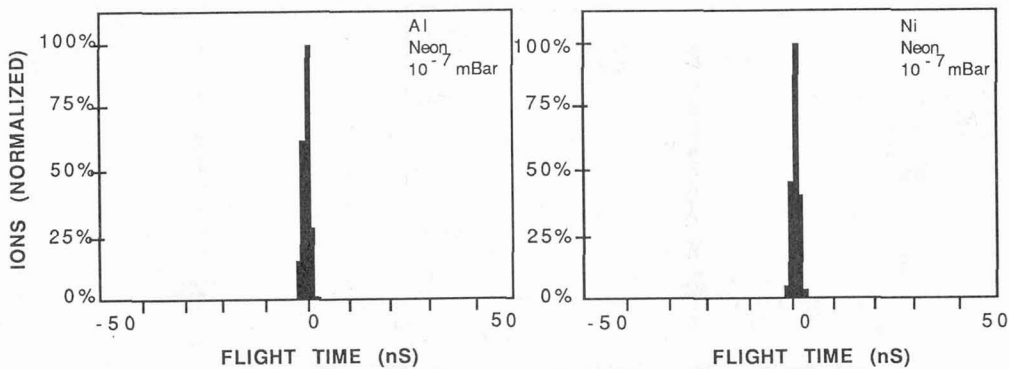


Fig. 3. Normalized Al^{1++} and $^{58}\text{Ni}^{1++}$ peaks in a time spectrum taken with a small beam divergence.

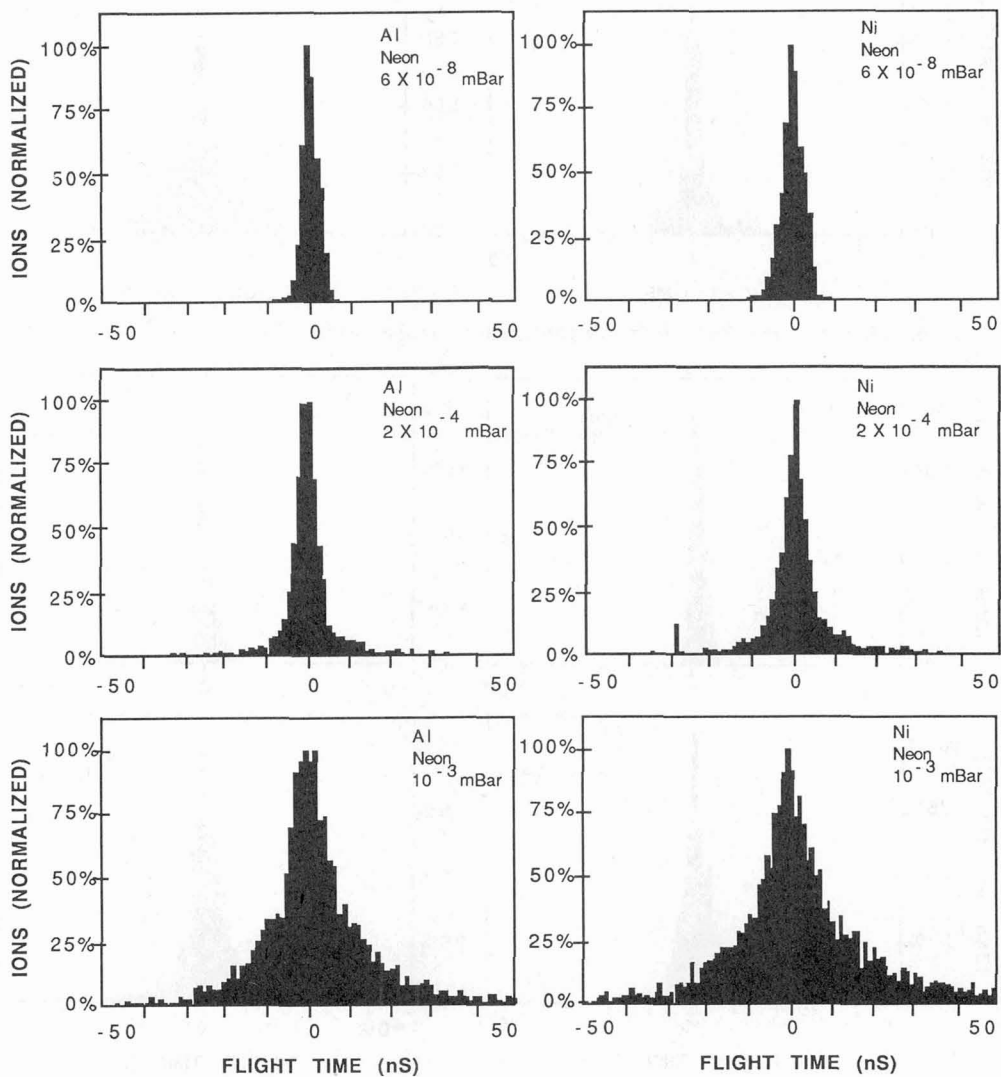


Fig. 4. Normalized Al^{1++} and $^{58}\text{Ni}^{1++}$ peaks in a time spectrum obtained under different neon image gas pressures.

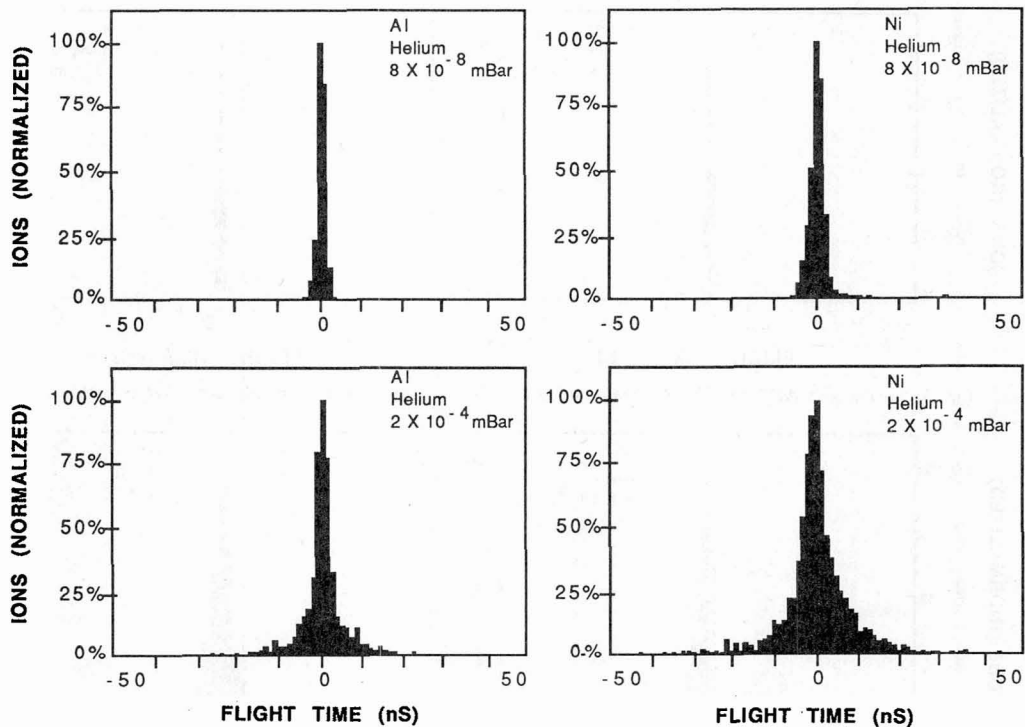


Fig. 5. Normalized Al⁺⁺ and ⁵⁸Ni⁺⁺ peaks in a time spectrum obtained under different helium image gas pressures.

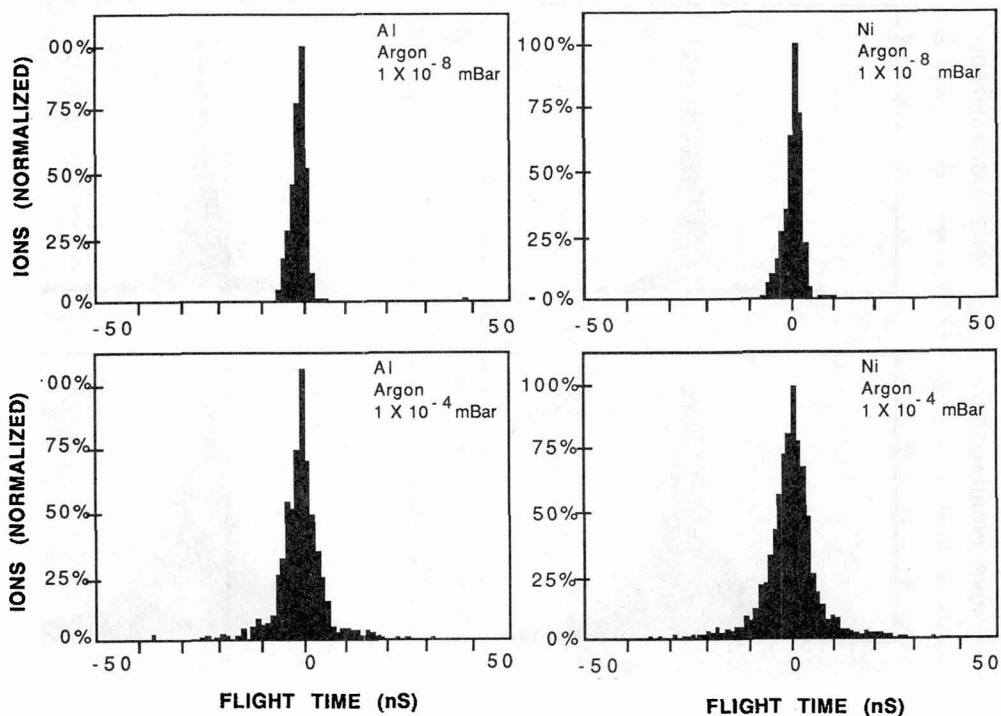


Fig. 6. Normalized Al⁺⁺ and ⁵⁸Ni⁺⁺ peaks in a time spectrum obtained under different argon image gas pressures.